J Sol-Gel Sci Techn (2006) 40:75–82
DOI 10.1007/s10971-006-8987-1

Effect of preparation conditions on the optical and physical properties of an epoxy-functional inorganic-organic hybrid material system

Mehmet Çopuroğlu · Shane O'Brien · Gabriel M. Crean

Received: 13 February 2006 / Accepted: 28 April 2006 / Published online: 15 July 2006

Abstract A hybrid material system consisting of (3-glycidyloxypropyl)trimethoxysilane, dimethyldimethoxysilane and zirconium(IV) *n*-propoxide was prepared. The influence of processing parameters including Zr content, UV irradiation and sol ageing on the properties of the resultant thin films was discussed. Refractive index, at 633 nm, and reflectance measurements were performed and near-field waveguide images of the samples were taken. Optical propagation loss measurements, at 633 nm, were studied. Film thickness and cross-sectional scanning electron microscopy images were obtained as a function of process conditions. FT-IR spectroscopy was used to monitor chemical reaction pathways in the system during processing. It was demonstrated that the crosslinking of epoxy groups in the structure, along with inorganic network formation as a result of sol-gel reactions, was the primary reason for the changes in the optical and physical properties of the system. As Zr containing species and/or UV irradiation may be employed to crosslink the epoxy groups in the structure, the optical and physical properties of the system can be tuned by optimal combination of these two crosslinking methods, as well as sol ageing process.

Keywords Sol-gel method · Organically modified silane · Crosslinking · Refractive index · Thickness · Waveguiding

M. Çopuroğlu · S. O'Brien · G. M. Crean (✉)
Tyndall National Institute,
Cork, Ireland
e-mail: gabriel.crean@tyndall.ie

G. M. Crean
Department of Microelectronic Engineering, University College
Cork, Ireland

1. Introduction

Inorganic-organic hybrid sol-gel based material systems play an important role in the development of optical waveguiding devices and are of considerable interest for possible photonic interconnect and sensor applications [1–7]. The sol-gel method has several advantages over conventional methods such as chemical vapour deposition or flame hydrolysis deposition to obtain such materials [8, 9].

Inorganic-organic hybrids with crosslinkable functional groups, such as acrylate or methacrylate are most commonly used at present [10]. An advantage of epoxy-based systems is that, crosslinking of the epoxy functional groups can be achieved either by a suitable catalyst or by irradiation with UV or visible light in the presence of a suitable photo-initiator [11, 12]. In addition to Si containing precursors, alkoxy compounds of transition metals such as Ti or Zr can also be involved in the sol-gel synthesis so that optical and physical properties can be tuned [10, 11, 13]. This is typically performed in order to optimise the refractive index of the cladding region in a planar waveguide device in order to minimize insertion losses. Currently Zr is the dopant of choice, as its reactivity can be more carefully controlled via complexation reactions, than that of Ti. Therefore, the compatibility of Zr dopant with epoxy-functionalised inorganic-organic hybrid systems is of considerable interest.

In this study, an inorganic-organic hybrid thin film system, containing epoxy side chains, was synthesised via the sol-gel route with different Zr compositions. The influence of Zr content, UV irradiation and sol ageing on the optical and physical properties of the material system was evaluated. The comparative effects of Zr doping and UV irradiation on

resultant film microstructure and functional properties were detailed for the first time.

2. Experimental

2.1. Preparation

The following synthesis route was used: (3-glycidyloxypropyl)trimethoxysilane (GDPTMS) (Fluka) and dimethyldimethoxysilane (DMDMOS) (Fluka) were mixed in a mass ratio of 9:1, respectively, to form the main inorganic structure. Various amounts of the mixture of zirconium(IV) *n*-propoxide ($Zr(OPr^n)_4$) (Fluka), a network former, a refractive index modifier and a catalyst for epoxy crosslinking, and methacrylic acid (MAA) (Merck) (with a mass ratio of 1:1) were added to the former mixture while stirring. $Zr(OPr^n)_4$ was stabilised with MAA to prevent the particulation of Zr as ZrO_2 due to the higher reactivity of Zr-alkoxides when compared to that of Si-alkoxides. After 30 min, aqueous HCl solution (0.1 M) and isopropanol, with a mass ratio of 9:2:1.6, GDPTMS:aqueous HCl solution:isopropanol, were added while stirring. After 1 h triarylsulfonium hexafluoroantimonate salts (50% mass in propylene carbonate) (Aldrich) were added to the system as a photo-initiator with a mass ratio of 1:0.1, GDPTMS:photo-initiator. After a further 1 h stirring, several samples were stored to investigate the effect of sol ageing at ambient conditions up to 240 h. The remaining samples were filtered to remove any unintended particulates by passing the sol-gel mixture through a 0.45 μm polypropylene Whatman™ filter. These samples were then spin-coated onto silicon wafer substrates using a WS-400A-6NPP/LITE Spin-Coater (Laurell Technologies Corp.) at a spin rate of 800 rpm for 30 s. Coated substrates were then dried on a hot-plate at 75°C for 30 min. Subsequently, several samples were irradiated with UV light up to 10 min using a DEK 1600 UV Exposure System to determine the influence of UV exposure time. The intensity of the UV source was 0 mW/cm^2 at 220 nm, 0.11 mW/cm^2 at 254 nm, 5.0 mW/cm^2 at 365 nm, and 14.2 mW/cm^2 at 400 nm. This range was suitable to activate the photo-initiator used in this study. Several samples were irradiated through a chrome-on-quartz contact mask for waveguide fabrication. All of the samples were again heated on a hot-plate at 75°C for 30 min. All samples were processed in the same manner. A schematic representation of this route is given in Scheme 1.

2.2. Characterisation

All refractive index measurements were performed at 633 nm using a Metricon 2010 Prism Coupler. The average of 15 measurements was used. The maximum deviation was ±0.001. A Tencor Alphastep 500 Surface Profiler was used to determine the film thickness. The reflectance of the sol-gel films was measured with a Shimadzu 2401 PC UV/Vis spectrophotometer. Changes in chemical functionality due to modification of the sol-gel film during process steps were monitored using a Varian FTS 7000 FT-IR spectrometer. Cross-sectional scanning electron microscopy (SEM) of the sol-gel films was performed using a Hitachi S-4000 Field Effect SEM instrument. Near-field images of the guided light output from the waveguides were obtained using a CCD camera. Optical propagation loss measurements were carried out at 633 nm using a DALI E-2100 device alignment instrument, with values calculated using the cleave-back method.

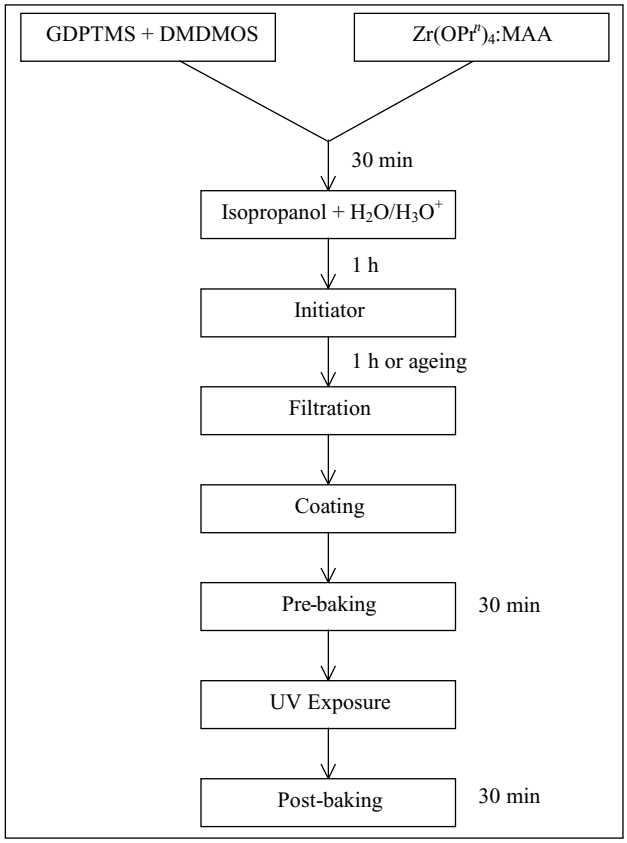

Scheme 1 The schematic representation of the preparation route followed

3. Results and discussion

A UV/Vis spectrum of a representative prepared sol-gel film (0.00 mol% Zr, UV-exposed (5 min) and unaged) is given in Fig. 1(a). It was observed, for all samples, that the reflectance is uniform over the visible range. An FT-IR spectrum of a representative prepared sol-gel film (11 mol% Zr, unexposed and aged for 96 h) is given in Fig. 1(b). The assignments of the generic peaks were made as follows: the broad peak

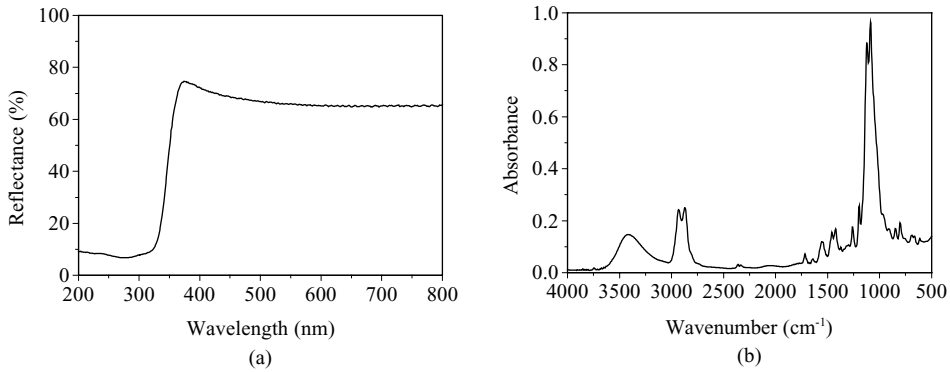

Fig. 1 UV/Vis (a) and FT-IR (b) spectra of the representative prepared sol-gel films

centred at 3414 cm^{-1} was assigned to O–H bonds; the features at 2870 and 2932 cm^{-1} were assigned to C–H bonds; the strong peak centred at 1107 cm^{-1} was assigned to Si–O bonds. In addition, the peak at around 1261 cm^{-1} was assigned to Si–CH_3 species [14], that at 760 cm^{-1} was assigned to the epoxy rings [15] and that at 613 cm^{-1} was assigned to Zr–O species [16]. The peak at around 1261 cm^{-1} was employed as a reference peak to be used in the evolution FT-IR spectra. It was assumed that the number of Si–CH_3 bonds remained constant during the synthesis. The relative changes, therefore, at any other wavenumber was monitored, by normalising the absorbance at that wavenumber to that of the Si–CH_3. Data processing was performed with appropriate baseline corrections.

3.1. Effect of Zr content and UV irradiation

The influence of Zr content on the physical and optical properties of both the unexposed and the UV-exposed (5 min) sol-gel films was investigated. Figure 2(a) and (b) show the variation of refractive index and thickness, respectively, as a function of Zr content. An increase in the refractive index of the unexposed system with increasing Zr content was observed. This may be attributed to two factors; firstly the high polarisability and large atomic size of Zr [13, 17, 18], and secondly, the catalytic effect of Zr on epoxy crosslinking [11]. The latter is more pronounced in the early stages of Zr doping, up to around 2 mol% Zr. A similar increase was observed in the refractive index of the UV-exposed system with increasing Zr content. However, the refractive indices of the UV-exposed samples, between 0 and approximately 11 mol% Zr, are higher than those of unexposed samples. It is suggested that UV-induced epoxy crosslinking [12] leads to this additional increase. This difference in refractive indices between the unexposed and UV-exposed samples became smaller as the Zr concentration increased and disappeared at approximately 11 mol% Zr concentration (Table 1). It is suggestive of a minimum Zr concentration at which all the epoxy crosslinking reactions are carried out by the catalytic effect of Zr. The relatively low refractive indices of the UV-exposed samples, with Zr contents ranging between 0.35 and approximately 2 mol% result from the fact that both Zr- and UV-induced epoxy crosslinking, in this concentration range, play an active role in determining the refractive index of the system. As the UV irradiation occurred after the film structure was partially crosslinked by the catalytic effect of Zr, the epoxy crosslinking potential of the UV irradiation decreased. The thickness of both the unexposed and the UV-exposed samples increased with increasing Zr content up to

Table 1 Variation of Δn with Zr content. (Δn: Difference in the refractive indices of unexposed and UV-exposed samples)

	Zr Content (Mole%)								
	0.00	0.35	0.70	1.2	1.7	3.4	6.6	11	17
Δn	0.017	0.010	0.009	0.008	0.005	0.004	0.003	0.000	0.001

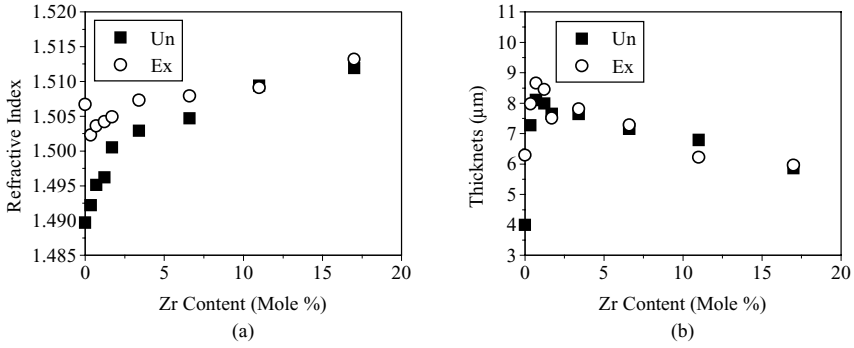

Fig. 2 Variation of refractive index (a) and thickness (b) with Zr content (Un: Unexposed, Ex: UV-exposed)

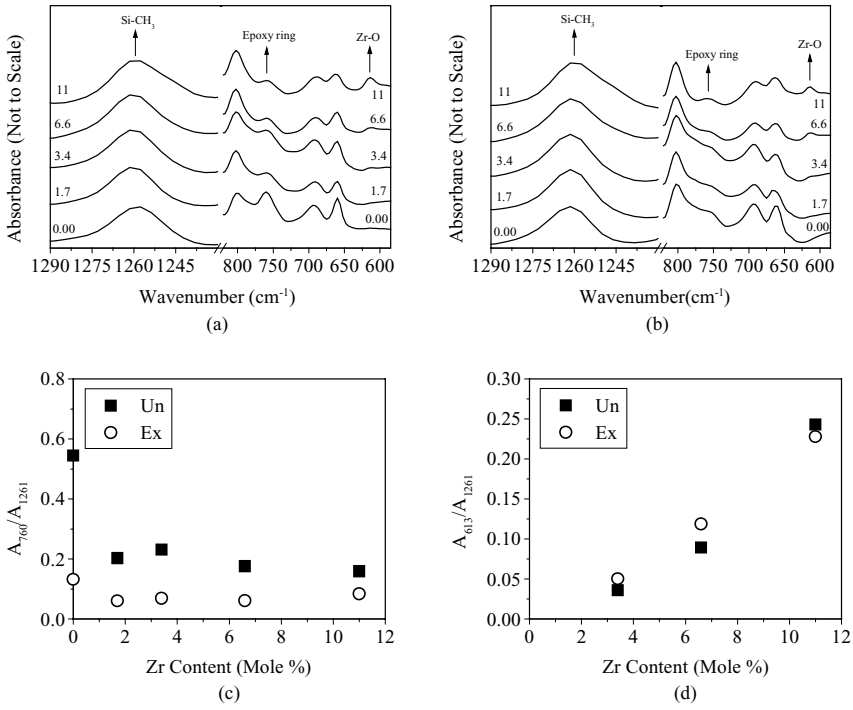

Fig. 3 Evolution FT-IR spectra of the unexposed (a) and UV-exposed (b) samples; and variation of the relative number of epoxy rings (c) and Zr-O species (d) as a function of Zr content doped. (Numbers on the curves correspond to the Zr content doped (mole%))

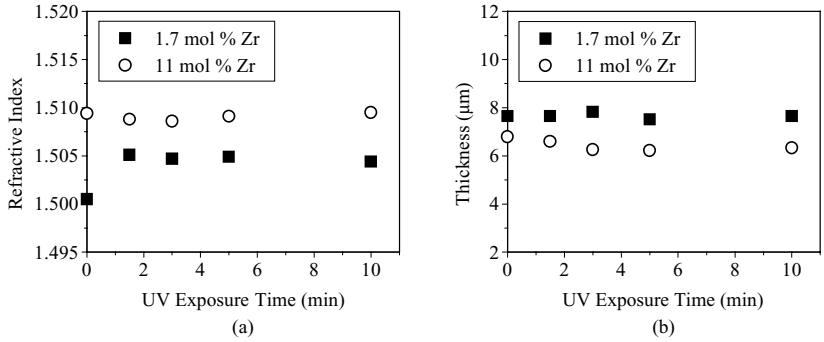

Fig. 4 Variation of refractive index (a) and thickness (b) with UV exposure time

around 2 mol%. Since this is the concentration range in which the epoxy crosslinking is more pronounced, this crosslinking leads to the formation of the main organic network structure, which then causes an increase in the thickness of the film. The thickness of the UV-exposed sample with 0.00 mol% Zr, however, is much less than that observed around 2 mol% Zr despite the high degree of crosslinking. This is possibly due to the fact that the epoxy crosslinking, in this case, is carried out only by UV light. This one-step crosslinking possibly leads to the formation of a more densely organically crosslinked network structure, which in turn causes volume shrinkage [10, 19]. In the case of UV-exposed samples, with Zr content ranging between 0.35 and approximately 2 mol%, crosslinking is carried out both by the catalytic effect of Zr and also by the UV-irradiation. The network, formed by this two-step crosslinking, is possibly less densely organically crosslinked, which results in less shrinkage. Above 2 mol% Zr the thickness was observed to decrease monotonically. This decrease was most likely the result of the relative dilution of epoxy groups in the structure with increasing Zr content, which therefore caused a decrease in the relative amount of organic crosslinks.

The above explanations are ascribed, in general, to the epoxy crosslinking reactions carried out by either the catalytic effect of Zr or the UV irradiation. In order to investigate the hypothesis, the relevant regions of the FT-IR spectra of the unexposed and UV-exposed samples were monitored and are given in Fig. 3(a) and (b), respectively. The decrease in the absorbance at around 760 cm^{-1}, for both unexposed and UV-exposed samples, supports the hypothesis. The relative amount of epoxy rings in the structure was also determined using the ratio of IR absorbance at 760 cm^{-1} (A_{760}) to that at 1261 cm^{-1} (A_{1261}), plotted as a function of Zr content. The change in the relative amount of epoxy rings with Zr

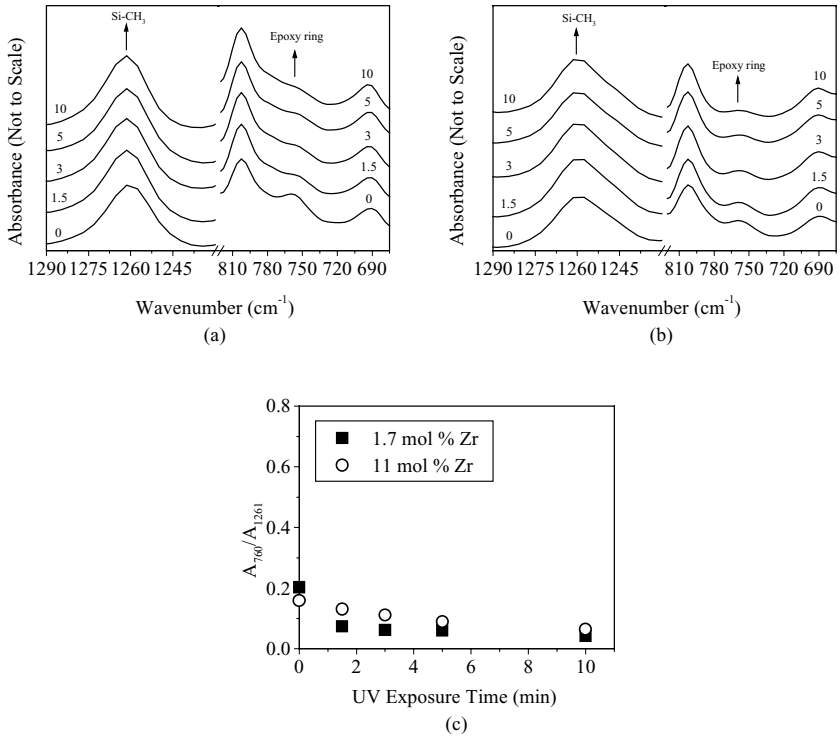

Fig. 5 Evolution FT-IR spectra of the sample sets with 1.7 (a) and 11 (b) mol% Zr; and variation of the relative number of epoxy rings (c) as a function of UV exposure time (Numbers on the curves correspond to the UV exposure time (minutes))

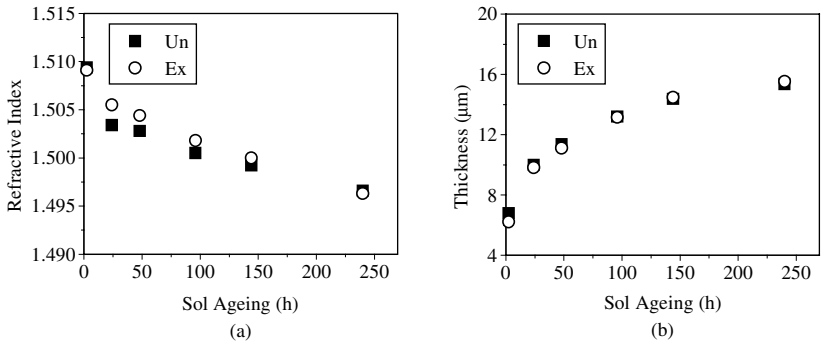

Fig. 6 Variation of refractive index (a) and thickness (b) with sol ageing. (Un: Unexposed, Ex: UV-exposed)

content (Fig. 3(c)), for both the unexposed and UV-exposed samples, is consistent with the explanations given above.

Figure 3(a) and (b) could also be used to show the presence of Zr in the resultant sol-gel films. The increase in the absorbance at around 613 cm^{-1}, for both the unexposed and the UV-exposed samples demonstrated that Zr was indeed present in the final film material. This increase, which manifests itself after approximately 3 mol% Zr, can also be followed from the ratio of IR absorbance at 613 cm^{-1} (A_{613}) to A_{1261} as a function of Zr content (Fig. 3(d)).

3.2. Effect of UV exposure time

The influence of UV exposure time was investigated for two representative sample sets, containing 1.7 and 11 mol% Zr. Figure 4(a) and (b) show the variation of refractive index and thickness, respectively, as a function of UV irradiation time. The refractive index of similar sol-gel hybrid materials was shown to increase with increasing UV exposure time [13, 20]. For the material systems in this study, this effect can only be taken into account in the samples with low Zr content, as epoxy groups in the structure will be already crosslinked by the catalytic effect of Zr before UV irradiation, for the samples with high Zr content. Therefore increasing the Zr content in the system decreases the potential UV-induced epoxy crosslinking effect. The refractive index of the hybrid system, at 11 mol% Zr, remains unchanged at all UV irradiation times, consistent with this explanation. UV irradiation of the sample, with 1.7 mol% Zr, for 1.5 min is sufficient to achieve the maximum refractive index of this material system. The thickness of samples at 1.7 and 11 mol% Zr

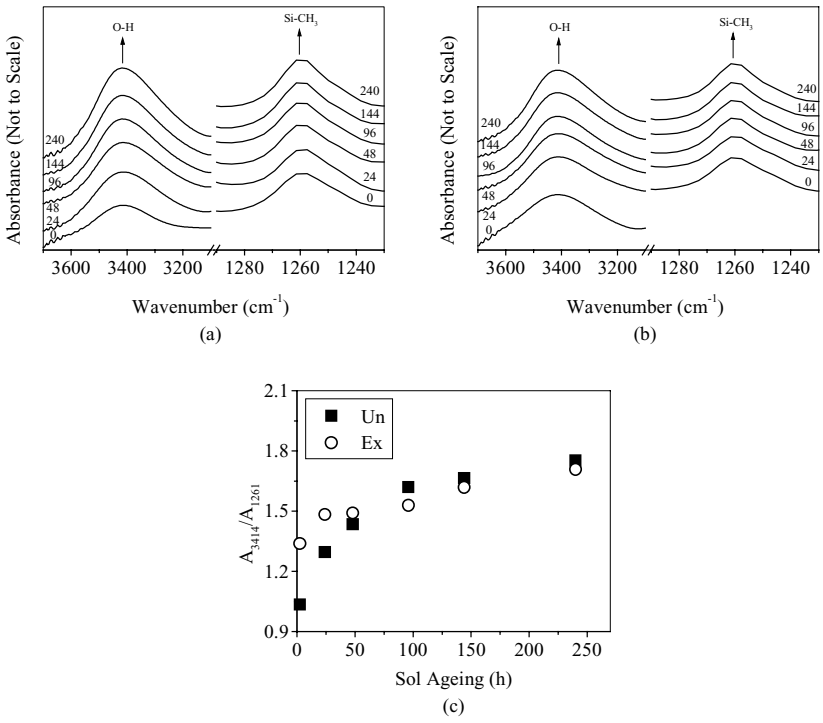

Fig. 7 Evolution FT-IR spectra of the unexposed (a) and UV-exposed (b) samples; and variation of the relative number of -OH groups (c) as a function of sol ageing. (Numbers on the curves correspond to the sol ageing time (hours))

content were not influenced by UV exposure time. This is most probably due to the main network structure being already in place before the samples were irradiated with UV light. The thickness of the sample with 1.7 mol% Zr content is higher than that of the sample with 11 mol% Zr content at all UV irradiation times. This is consistent with the relative dilution of epoxy groups with increasing Zr content in the structure.

In order to track the progress of epoxy ring opening reactions upon UV irradiation, the relevant regions of the FT-IR spectra of the samples with 1.7 and 11 mol% Zr content were monitored and are given in Fig. 5(a) and (b), respectively. The decrease in the absorbance at around 760 cm^{-1}, consistent with the UV-induced epoxy ring opening, can be observed for both sample sets. The ratio of A_{760} to A_{1261} was also plotted against UV exposure time (Fig. 5(c)) as a function of UV irradiation time. This ratio slightly decreased with increasing UV exposure time for both sample sets. The ratios for both systems are low at all UV irradiation times. This is due to the fact that these material systems are already crosslinked, to a certain degree, before irradiation with UV light.

3.3. Effect of sol ageing

The influence of sol ageing on the material system, with 11 mol% Zr, for both the unexposed and the UV-exposed samples, was also investigated. Figure 6(a) and (b) show the variation of refractive index and thickness, respectively, with sol ageing. It was observed that increasing the sol ageing time decreased the refractive index of the system, both for unexposed and UV-exposed samples. This is consistent with the ongoing progress of hydrolysis and polycondensation (including homo- and heterocondensation of both Si and Zr containing species) reactions with time [21, 22]. In the early stages of the sol ageing process, because of weak branching combined with limited condensation and decreasing solvent concentration during film formation, precursors interpenetrate and the structure becomes densely packed and relatively less porous [23]. Therefore, the porosity of the structure increased with sol ageing, which in turn decreased the refractive index whilst also increasing the thickness of deposited films. This increase in film thickness suggested that the inorganic crosslinking was dominant over the organic crosslinking in determining the network structure of the system at 11 mol% Zr.

In order to demonstrate the progress of hydrolysis reactions with sol ageing, the relevant regions of the FT-IR spectra of the unexposed and UV-exposed samples were monitored and are given in Fig. 7(a) and (b), respectively. The increase in the absorbance at around 3414 cm^{-1} was attributed to the further hydrolysis reactions that occurred during sol ageing. The progress of the hydrolysis reactions during sol ageing can also be observed by monitoring the ratio of IR absorbance at 3414 cm^{-1} (A_{3414}) to A_{1261} as a function of sol ageing time (Fig. 7(c)). An increase was observed in the ratio A_{3414}/A_{1261} for both unexposed

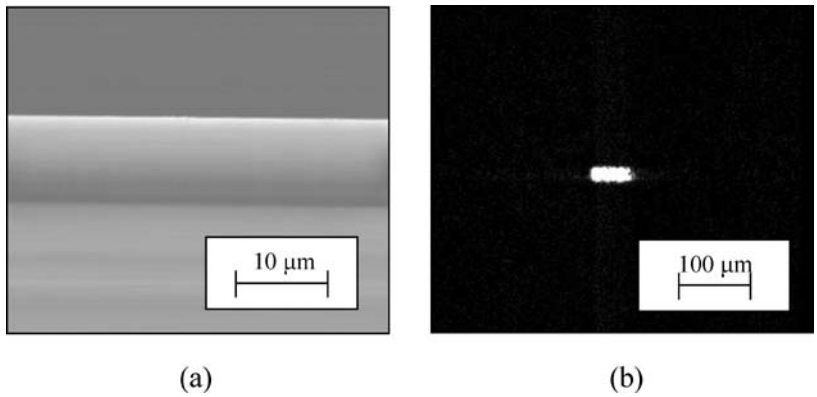

Fig. 8 A cross-sectional SEM image of a representative prepared sol-gel film (a), and a near-field image of the guided light output from a representative prepared waveguide (b)

and UV-exposed samples suggestive of further hydrolysis reactions during sol ageing. Nevertheless, the rate of increase reduced with sol ageing. This may be attributed to the saturation, in number, of Si–OH and/or Zr–OH species with sol ageing, and further condensation reactions, which therefore decreased the number of Si–O–R and/or Zr–O–R (where R is: methyl, or *n*- or *iso*-propyl) species, necessary for hydrolysis reactions.

3.4. SEM and near-field optical analysis

A cross-sectional SEM image of a representative prepared sol-gel film (6.6 mol% Zr, UV-exposed (5 min) and unaged) showed that the films can be obtained as crack-free (Fig. 8(a)). A near-field image of the guided light output from a representative prepared waveguide (0.00 mol% Zr, UV-exposed (5 min) and unaged) demonstrated that the light was confined to the core region of the waveguide (Fig. 8(b)). The measured minimum propagation loss of the guide was obtained from the same sample and found to be 0.8 dB cm^{-1}. This material system therefore appears suitable for potential short range photonic interconnect and sensing applications.

4. Conclusion

A novel inorganic-organic hybrid system with epoxy functionality was prepared by the sol-gel method. The optical and physical properties of the materials were characterised as a function of process variables including Zr content, UV irradiation and sol ageing.

It was shown that both the refractive index (at 633 nm) and thickness of the material system could be tuned by Zr doping and/or UV irradiation and/or a sol ageing process. The comparative epoxy crosslinking effects of Zr doping and UV irradiation were presented for the first time. Moreover, it was demonstrated that the crosslinking of epoxy groups, along with the inorganic network formation as a result of sol-gel reactions, is the main influence on the observed modifications in the optical and physical properties of the material system. As Zr containing species and/or UV irradiation may be employed to crosslink the epoxy groups in the structure, the combination of these two crosslinking methods provides a new process regime to obtain thin film materials with desired optical and physical properties.

Acknowledgments This work was supported by the Irish Government, Department of Education and Science through the Higher Education Authority Programme for Research in Third Level Institutions, Project Eco-Electronics.

References

1. Krug H, Tiefensee F, Oliveira PW, Schmidt H (1992) Sol-Gel Optics II, SPIE 1758:448
2. Buestrich R, Kahlenberg F, Popall M, Dannberg P, Müller-Fiedler R, Rösch O (2001) J Sol-Gel Sci Technol 20:181
3. Que W, Zhou Y, Lam YL, Chan YC, Kam CH (2001) J Sol-Gel Sci Technol 20:187
4. O'Brien S, Winfield RJ, Connell A, Crean GM (2005) In: Sanchez C, Schubert U, Laine RM, Chujo Y (eds), Organic/inorganic hybrid materials (Mater. Res. Soc. Symp. Proc. 847, Warrendale, PA), EE13.20.1
5. Wang B, Hu L (2006) Ceram Int 32:7
6. Luo X, Zha C, Luther-Davies B (2005) Opt Mater 27:1461
7. Que W, Hu X, Zhou J (2005) Thin Solid Films 484:278
8. Coudray P, Chisham J, Malek-Tabrizi A, Li C-Y, Andrews MP, Peyghambarian N, Najafi SI (1996) Opt Commun 128: 19
9. Coudray P, Etienne P, Moreau Y (2000) Mat Sci Semicon Proc 3:331
10. Haas K-H, Wolter H (1999) Curr Opin Solid State Mater Sci 4: 571
11. Philipp G, Schmidt H (1986) J Non-Cryst Solids 82:31
12. Crivello JV, Song KY, Ghoshal R (2001) Chem Mater 13: 1932
13. Zhang X, Lu H, Soutar AM, Zeng X (2004) J Mater Chem 14: 357
14. Que W, Hu X (2003) J Sol-Gel Sci Technol 28:319
15. Chiniwalla P, Bai Y, Elce E, Shick R, McDougall WC, Allen SAB, Kohl PA (2003) J Appl Polym Sci 89:568
16. López EF, Escribano VS, Panizza M, Carnasciali MM, Busca G (2001) J Mater Chem 11:1891

17. Oubaha M, Etienne P, Calas S, Coudray P, Nedelec JM, Moreau Y (2005) J Sol-Gel Sci Technol 33:241
18. Sorek Y, Zevin M, Reisfeld R, Hurvits T, Ruschin S (1997) Chem Mater 9:670
19. Schoch KF Jr, Panackal PA, Frank PP (2004) Thermochim Acta 417:115
20. Moujoud A, Saddiki Z, Touam T, Najafi SI (2002) Thin Solid Films 422:161
21. Brinker CJ, Scherer GW (1990) Sol-gel science: the physics and chemistry of sol-gel processing. Academic Press, San Diego, p 358
22. Zhang Q, Huang Z, Whatmore RW (2002) J Sol-Gel Sci Technol 23:135
23. Brinker CJ, Scherer GW (1990) Sol-gel science: The physics and chemistry of Sol-gel processing. Academic Press, San Diego, p 803